EUROFUSION WPJET1-CP(16) 15040

PC de Vries et al.

Multi-machine analysis of termination scenarios, providing the specifications for controlled shutdown of ITER discharges

Preprint of Paper to be submitted for publication in
Proceedings of 26th IAEA Fusion Energy Conference

This work has been carried out within the framework of the EUROfusion Consortium and has received funding from the Euratom research and training programme 2014-2018 under grant agreement No 633053. The views and opinions expressed herein do not necessarily reflect those of the European Commission.

This document is intended for publication in the open literature. It is made available on the clear understanding that it may not be further circulated and extracts or references may not be published prior to publication of the original when applicable, or without the consent of the Publications Officer, EUROfusion Programme Management Unit, Culham Science Centre, Abingdon, Oxon, OX14 3DB, UK or e-mail Publications.Officer@euro-fusion.org

Enquiries about Copyright and reproduction should be addressed to the Publications Officer, EUROfusion Programme Management Unit, Culham Science Centre, Abingdon, Oxon, OX14 3DB, UK or e-mail Publications.Officer@euro-fusion.org

The contents of this preprint and all other EUROfusion Preprints, Reports and Conference Papers are available to view online free at http://www.euro-fusionscipub.org. This site has full search facilities and e-mail alert options. In the JET specific papers the diagrams contained within the PDFs on this site are hyperlinked

Multi-machine analysis of termination scenarios, providing the specifications for controlled shutdown of ITER discharges

P.C. de Vries 1), T.C. Luce 2), Y.S. Bae 3), S. Gerhard 4), X. Gong 5), Y. Gribov 1), D. Humphreys 2), A. Kavin 6), R. Khayrutdinov 7), C. Kessel 4), S.H. Kim 1), A. Loarte 1), V. Lukash 7), E. de la Luna 8,9), I. Nunes 8,10), F. Poli 4), J. Qian 5), O. Sauter 11), A.C.C. Sips 8,12), J.A. Snipes 1), J. Stober 13), W. Treutterer 13), A. Teplukhina 11), I. Voitsekhovitch 14), M.H. Woo 3), S. Wolfe 15), L. Zabeo 1), the Alcator C-MOD team, the ASDEX Upgrade team, the DIII-D team, the EAST team, JET contributors 16), the KSTAR team, the NSTX-U team, the TCV team and ITPA IOS members and experts.

1) ITER Organization, Route de Vinon sur Verdon, 13067 St Paul Lez Durance, France.
2) General Atomics, PO Box 85608, San Diego, CA 92186-5608, USA.
3) National Fusion Research Institute, Daejeon, Korea.
4) Princeton Plasma Physics Laboratory, Princeton University, Princeton, NJ 08543, USA.
5) Institute of Plasma Physics, Chinese Academy of Sciences, Hefei 230031, P.R. China.
6) D.V. Efremov Institute of Electrophysical Apparatus, Saint Petersburg, Russia.
7) National Research Center Kurchatov Institute, Moscow, Russia.
8) EUROfusion Consortium, JET, Culham Science Centre, Abingdon, OX14 3DB, UK.
9) Laboratorio Nacional de Fusion, CIEMAT, 28040 Madrid, Spain.
10) Associação EURATOM-IST, Instituto de Plasmas e Fusão Nuclear, Lisboa, Portugal.
11) École Polytechnique Fédérale de Lausanne (EPFL), Swiss Plasma Center (SPC), CH-1015, Switzerland
12) European Commission, Brussels, Belgium.
13) Max-Planck-Institut für Plasmaphysik, 85748 Garching, Germany.
14) CCFE, Culham Science Centre, OX14 3DB Abingdon, UK.
15) Plasma Science and Fusion Center, MIT, Cambridge, MA, USA.
16) See the Appendix of F. Romanelli et al., Proc. of the 25th IAEA FEC 2014, St Petersburg, Russia
E-mail: Peter.Devries@iter.org

1. Introduction

The controlled shutdown is an often overlooked, though important, phase of the tokamak discharge. The dynamics during this phase complicate control, making it difficult to avoid operational limits, which in the worst case, may lead to a disruption. This is exacerbated by the fact that at the end of the discharge, the device is usually operating close to its technical limits. For unplanned terminations, triggered by off-normal events, the situation complicates further. The ability to carry out a well-controlled termination contributes significantly to the avoidance of disruptions.

To improve our understanding of the dynamics and control of ITER terminations, a study has been carried out on data from existing tokamaks. The aim of this joint analysis is to compare the assumptions for ITER terminations with the present experience basis. The study examined the parameter ranges in which present day devices operated during their terminations, as well as the dynamics of these parameters. The dynamics may vary considerably over the duration of the termination hence, simply comparing average values may not always be sufficient. Moreover, sometimes the dynamics of different parameters are coupled. The analysis addresses changes in plasma shape and internal inductance, ℓ_i, during the plasma current ramp-down, relevant to vertical stability (VS) control, the energy (or, the poloidal β: β_p) decay, which relates to the radial position control, and the controllability of the both density decay and the H to L-mode back transition. Typical time scales, such as the energy confinement time and the L/R time do not have a fixed ratio from device to device, complicating the extrapolation of the termination scenario results. This paper will first describe, in section 2, the specifics of discharge terminations in ITER, giving the main restrictions and control aspects. Then, in section 3, the database of terminations from Alcator C-Mod, ASDEX Upgrade, DIII-D, EAST, JET, KSTAR, NSTX/NSTX-U and TCV is presented. The database also contains a number of simulated ITER terminations. This is followed by a comparison of the stability aspects (section 4) and dynamics of a number of key parameters (section 5). The results from the joint analysis can be used to better prescribe the inputs for the modelling and the further preparation of ITER termination scenarios.

2. ITER termination scenarios: restrictions and example

The termination phase should achieve a simultaneous ramp-down of the plasma current, kinetic energy and particle density while maintaining control over the radiation levels, plasma position and shape (i.e. avoid overheating the first wall) and VS, staying within the capabilities of the poloidal field coils and power supplies and heating systems. Stability boundaries and general operational limits must also be avoided. ITER will operate at high densities and a controlled density decay is important to avoid the density limit, while also managing the H-L transition timing and exit from fusion burn. ITER power supply limitations and the thick vessel slow the control response for vertical stability (VS) and the radial position. Previously, experiments on discharge terminations focused mainly on the electromagnetic changes and on the controllability of vertical stability [1-3]. It was found that VS control could be maintained in ITER by restricting the increase in internal inductance ℓ_i (e.g. by keeping the temperature high) and reducing the elongation, κ. Changes to the shape are obviously restricted by the PF coil limits but for large elongation changes the power flow diverted to the upper part of the blanket and the position of upper strike points need to be controlled. In ITER, plasmas heated by auxiliary power should remain diverted, while at currents of I_p~7.5MA or above, the blanket can only sustain Ohmic power for a short time (~a few secs). A fast drop in β_p during the H-L transition, may result in an uncontrolled inward radial motion. This means the plasma could touch the inner wall or become less vertically stable as it loses its proximity to the vessel.

There is no single solution to overcome these issues for ITER terminations. The design of a termination scenario can place different weights on each restriction, e.g. reducing the plasma volume allowing a larger radial excursion, hence a larger drop in β_p. These weights also depend on the goal of the termination. A normal ITER termination, should aim to be in full control until the current is below I_p=3MA, when the direct disruption impact is expected to be benign [4], and even lower when runaways are considered. The goal for an emergency termination is different, aiming for a fast reduction of current and energy, with the knowledge that control will be lost and the plasma may disrupt, although with a smaller impact [5]. Studies have also been carried out on the fastest ITER exits from full performance, i.e. by direct switch off of auxiliary heating [6]. The fastest ITER current ramp-down is limited by the PF coil voltages and the requirements to control (shape, position and VS stability) with a certain precision. In ITER, a fully controlled current ramp-down from I_p=15MA to below I_p=1MA can be achieved in ~60s. An example of a typical ITER termination, modelled with the Corsica code, is shown in figure 1. The current ramp-down has a duration of 210s, with a moderate current ramp-down rate of 0.07MA/s. At the start of the termination the plasma is still in H-mode and at full performance, with an α-power of P_α=100MW (Q=10) and a kinetic energy of W_{kin}=350MJ. The input power decays relatively quickly, mainly due to the fast decrease in α-power, as the auxiliary power and current are reduced.

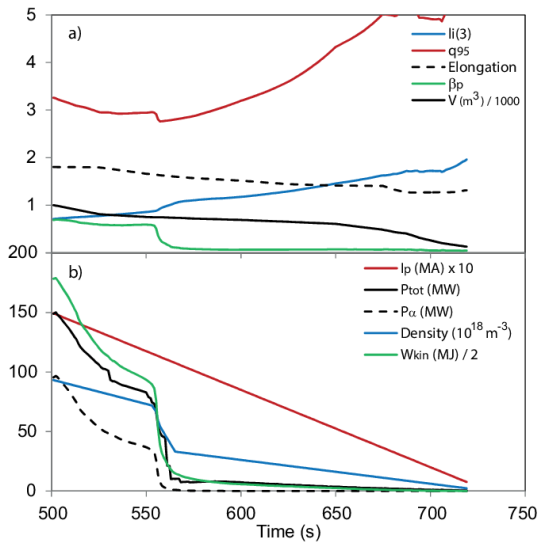

FIG. 1: *A modelled ITER termination (Corsica Hmode_15MA_13) from I_p=15MA at full performance (W_{kin}=350MJ, P_α=100MW).*

The H-L transition already takes place at t~570s, i.e. 70s after the start of the termination. The model has to make an assumption for the duration of this transition, here less than 10s. Similarly the decay of the density is assumed such that the Greenwald-fraction remains constant, with a jump at the time of the H-L transition. Figure 1a, shows the rather large drop in β_p at the time of this transition which in this case avoids too large a radial movement. Especially during the L-mode phase, ℓ_i increases considerably, but VS is ensured by a reduction in plasma volume in the first 20s of the termination, followed by a steady reduction of κ and volume. The volume reduction also allows for a larger radial movement at the time of the H-L transition. As a consequence of this volume change, q_{95} remains around 3 for almost half of the current ramp-down (i.e. up to t~600s), only to increase afterwards.

3. Database of tokamak terminations

A database has been created consisting of typical, special and ITER-like, terminations from Alcator C-Mod, ASDEX Upgrade, DIII-D, EAST, JET, KSTAR, NSTX/NSTX-U and TCV. Hence, there are examples from devices with full metal walls that can be compared with those with carbon walls, and two devices that, like ITER, have super-conducting coils. Wide ranges of heating schemes were used in the database terminations. DIII-D, JET and TCV provided also ohmic terminations, although the emphasis of the analysis presented in this paper is on the termination from H-mode.

These can be directly compared with four modelled ITER terminations; one termination with a moderate duration (shown in figure 1), two fast terminations modelled by the DINA code, with a duration of 60 and 68s, and finally, a DINA simulation of a hypothetical slowest possible termination, in which the plasma current decays naturally while being kept in H-mode, lasting 1100s. In the paper, this entry is identified, separately from the other ITER cases, by a black border around its orange diamond. For some database entries, certain parameters were not provided, therefore, these are missing from some figures in the paper.

In figure 2, a comparison of a number of characteristic time-scales is presented. The average current ramp-down for each database entry is shown, in figure 2a, as a function of the inductance, L, for each device, here calculated as: $\mu_o r_o(\ln(8r_o/a)-2-\ell_i/2)$, where r_o and a are the major and minor radius, respectively, and assuming $\ell_i=1$ The average ramp-down time is here defined as the time integrated value of the parameter, divided by half the value at the start of the termination. Figure 2b shows that for larger devices the current ramp-down time is generally a smaller fraction of the L/R time (with R the plasma resistance), $\tau_{L/R}$, here averaged over the first half of the current decay. The resistance for each entry is determined as P_{ohmic}/I_p^2, except for TCV for which Spitzer resistivity is assumed, using temperature and Z_{eff} data. The L/R time, $\tau_{L/R}$, is the characteristic time of a natural plasma current decay. This differs from the resistive time, τ_R, being the typical time scale to achieve an equilibrium internal current density, thus related to changes in ℓ_i [6,7], as will be discussed in section 5.

Figure 2c shows the average input power ramp-down time, normalized to that of the current. Those terminations in present day devices, carried out to show how to limit the increase in ℓ_i, have relatively long power ramp-downs, i.e. the ratio with the current ramp-down is >0.8. But, for typical ITER terminations, the power ramp-down, and consequently the decay in thermal energy, is relatively fast. The reason is that a large fraction is due to α-power. It is therefore not easy to maintain H-mode over a large part of the current decay in ITER. Of course this differs for ITER terminations with a smaller fraction of α-power, for example at lower current. Similar analysis of the average ramp-down of the density is relatively slow, for most entries. The behavior of the density during the termination is analyzed in more detail in section 5.

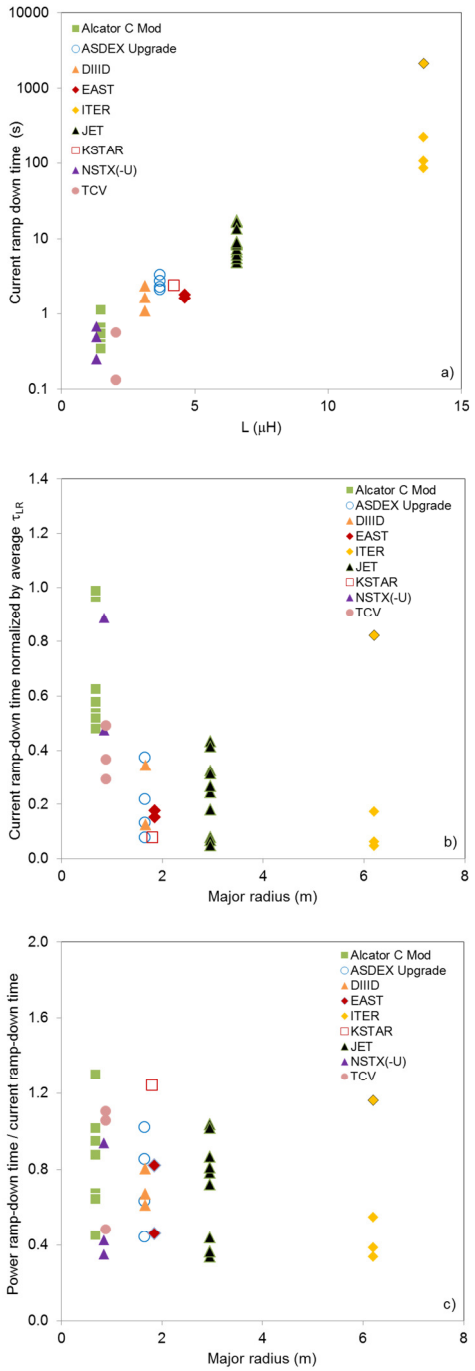

FIG. 2: *Existence diagrams of database entries showing a) the current ramp-down time versus the device inductance, L, b) the current ramp-down time normalized to $\tau_{L/R}$, versus major radius c) the relative power ramp-down time versus major radius.*

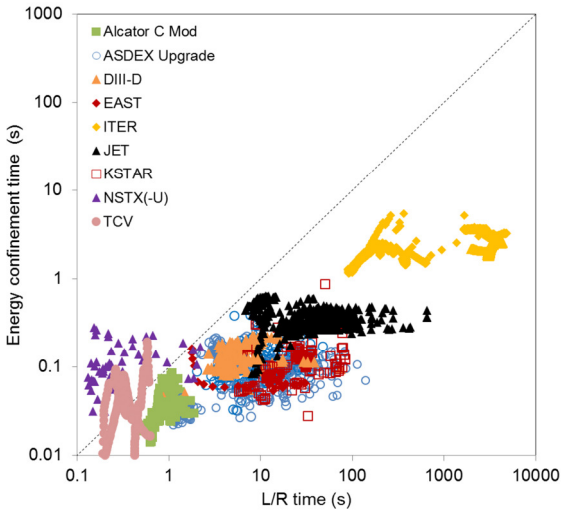

FIG. 3: *The energy confinement time, τ_E, versus the L/R time, $\tau_{L/R}$, for each time step during a number of database terminations in devices of different size.*

The average ramp-down times allow only a rough comparison but do not capture the variation in dynamics that may take place during a termination, such as a fast H-L back transition. For this purpose one can simply plot values of interest at each time step. Each termination in the database contains data with approximately 150-200 time steps.

This has been used to create figure 3, comparing the energy confinement time, τ_E, and $\tau_{L/R}$. The variation in τ_E, is limited, per device, but also over the duration of the termination, while, $\tau_{L/R}$, often varies over several orders of magnitude. Therefore, it is difficult to match a single value of $\tau_{L/R}$ to each termination case. Figure 3 also shows that ratio of τ_E to $\tau_{L/R}$ varies from device to devices, leading to a different scaling of kinetic and electromagnetic dynamics.

4. Comparison of stability aspects

Maintaining VS is an important aspect for a termination. The VS of the plasma depends on a complex function of ℓ_i, β_p and elongation κ, and, furthermore, on the proximity of the plasma to stabilizing passive components, such as the vacuum vessel in ITER, and on the capability of the VS control circuit. The latter factors differ from device to device and this does not make a comparison straightforward. Figure 4a show the typical traces in κ, and ℓ_i space that each database entry follows during a termination. The reduction in κ that is applied by the ITER cases is relatively large and its data points lie on the edge of the space spanned by the other devices. The complex relationship between vertical instability ℓ_i, β_p, κ, can be expressed by the so-called marginal stability parameter, defined as [9,10]:

$$m_s = \left[\frac{1.47\,(1+e^{-2l_i+1})}{2(\kappa-1.13)} - 1\right](1 + 0.6(\beta_p - 0.1)) \qquad (1)$$

The lower m_s is, the more unstable the plasma, although the critical point for VS is device specific. Figure 4b, shows the values of m_s during the terminations in the database.

In most cases, but not all, the value increases with time (i.e. becomes more stable). The minimum value, at which VS is lost varies from device to device. In ITER it depends on the vertical stability

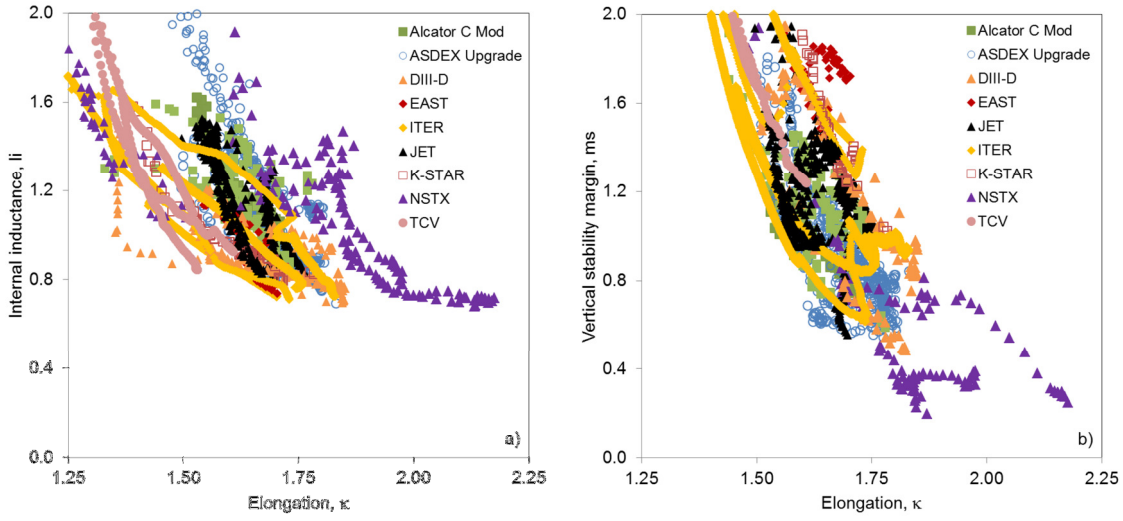

FIG. 4: *a) The traces in the κ- ℓ_i operational space. b) The marginal stability parameter, m_s, during the termination of all database entries. Note in both cases the outlying highly elongated NSTX cases.*

control circuits that are used, ranging from roughly m_s~0.15 to ~0.25 when, respectively, VS3 (also using in-vessel coils) or only VS1 (only the ex-vessel coils) are used. The modelled ITER cases often fall near the edge of the experimental cases, because these assume a faster and larger reduction in κ than used by most devices. For the more standard ITER terminations, m_s>0.8, although the slow natural current decay in H-mode achieves a minimum value m_s~0.6, because the plasma shape is not modified in this case. Except for the very low values found for highly elongated NSTX terminations, lowest values in standard aspect ratio devices are always found above m_s~0.4.

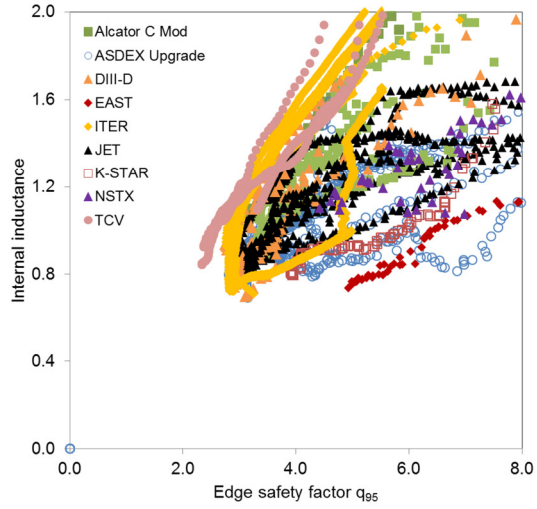

FIG. 5: The traces of each entry in ℓ_i-q space.

The well-known ℓ_i-q stability diagram, shown in figure 5, provides another view into the stability of the termination. The result of the fast reduction in κ and volume is, that the modelled ITER terminations, remain much longer at q_{95}~3, as shown earlier in figure 1, and thereafter trace the upper boundary spanned by the experimental data. This does not necessarily mean that this track is more unstable. However, other devices often show an earlier increase to higher q_{95}, which is especially true for those that keep the magnetic field constant during the current ramp-down, such as ASDEX Upgrade, TCV and super-conducting devices, EAST and K-STAR. The faster route to a higher q_{95} might be better with respect to MHD stability, but requires additional heating to avoid excessive ℓ_i.

5. Comparison of dynamics

While in most cases the current is ramped down at a constant rate, the decay rates of thermal energy, or β_p, density or Greenwald fraction f_{GW} will vary. Here f_{GW} is the average density (in 10^{20} m^3) normalized by the Greenwald density $n_{GW}=I_p/\pi a^2$ with I_p in MA and a in m) [11]. The decay of these parameters will differ between the H and L-mode phase, and fast changes are expected during the H-L transition itself.

In figure 6 the decay time of the energy and density is compared with that of the current. The decay time of parameter X is defined as the inverse decay rate, $-1/X \times dX/dt$. It shows that at times, the energy and especially density decay slower than the current, such that one obtains an increasing β_p ($\propto W/I_p^2$) and f_{GW}, ($\propto n/I_p$). The fastest energy and density decay, usually of the order of the

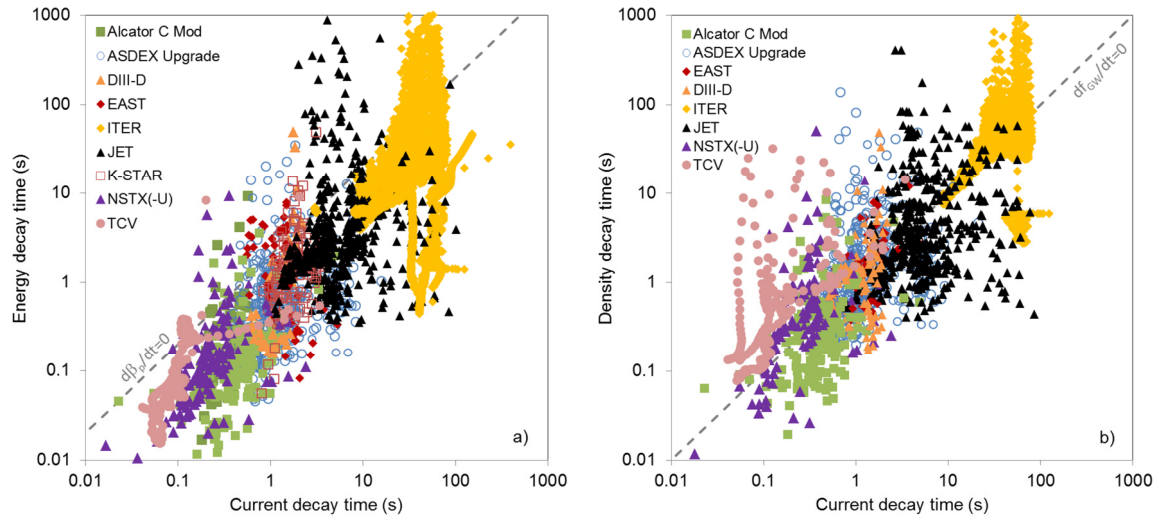

FIG. 6: *a) The energy decay rate compared to the current decay rate for each time step during the termination. Below the dashed line β_p decreases. b) The density decay rate compared to the current decay rate for each time step during the termination. Below the dashed line, f_{GW} decreases.*

the order of the energy confinement time, are found at the time of the H-L transition. Note that negative decay times (i.e. increases) are also possible but not visible in figure 6.

Figure 7 shows the typical changes in β_p and f_{GW} during the H-mode phase of the terminations. Both parameters tend to increase up to the H-L transition. The longer the power is maintained, and the plasma is kept in H-mode, the larger the increase in β_p and f_{GW}. After the H-L transition has taken place the same is true for the L-mode phase, when, in general β_p increases in time. It is not clear, so far, why the density decreases slower than the plasma current. No indication was found that the heating mixture matters with respect to the density decay. The auxiliary power composition varied for the database entries with some being purely neutral beam (NB) heated, others solely by radiofrequency (RF) heating, and some by a mixture of the two. Obviously, when the termination is started at an already high f_{GW}, one cannot keep the plasma in H-mode and simultaneously ramp-down the current for too long, before reaching the Greenwald density limit [11].

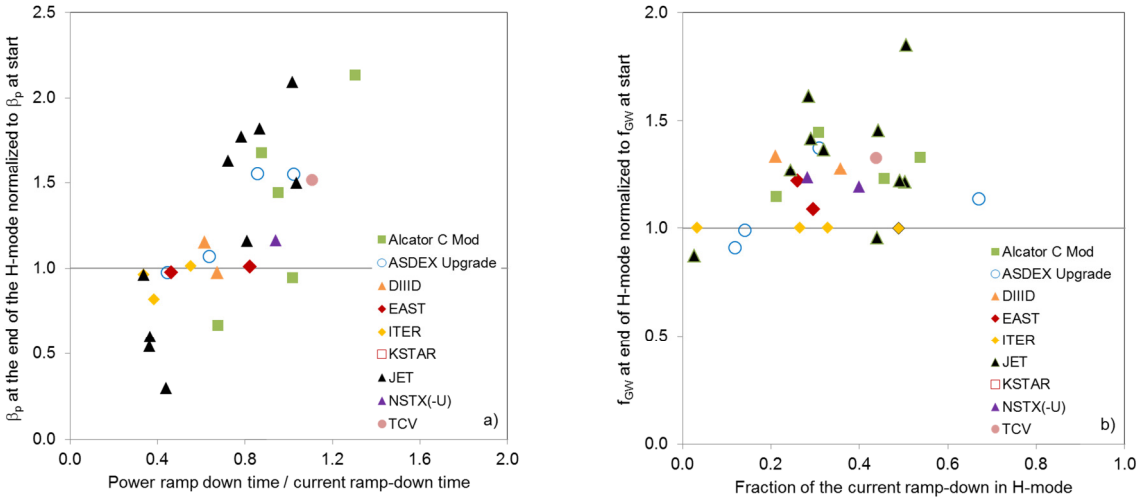

FIG. 7: *a) The change in β_p over the first part of the termination phase, up to the H-L back transition versus the ratio of power ramp-down time to current ramp-down time. b) The change in f_{GW} over the first part of the termination phase, up to the H-L back transition, versus of the fraction of the current ramp-down kept in H-mode. Note that the modelled ITER cases simply assume that f_{GW} remains constant.*

The H-L transition duration was determined by calculating the FWHM of the time derivative of β_p, over the transition. It was found that in all devices the duration lasted between 1.5-3×τ_E. The shortest transitions were found for those entries that had a high value of β_p prior to the transition. The magnitudes of the drop in energy, β_p, and f_{GW} over the H-L transition were determined. At many entries the peak energy decay time (i.e. the inverse W^{-1}×dW/dt) was found to be of the same order as τ_E (i.e. the energy derivative dominates the total input power at this specific moment in time). In figure 8, the peak changes in β_p and f_{GW}, normalized by τ_E, over the HL back transition are shown. The values are lower for those cases that gradually ramp-down the input power (i.e. the power at the HL transition is smaller with respect to the power at the start of the termination) or those that have a shorter H-mode phase with respect to the current ramp-down. As discussed above, longer H-mode phases, usually lead to high values of β_p and f_{GW}, just prior to the H-L transition. Typical values are $0.05<\tau_E\times|d\beta_p/dt|<0.85$ and $0.06<\tau_E\times|df_{GW}/dt|<0.60$. The experimental values can be compared to those assumed in the modelled ITER cases (see figure 8). The normalization by τ_E, being the characteristic time of the H-L transition process, allows a comparison between the various devices. However, τ_E is not the characteristic time that sets the allowed change in β_p with respect to the radial position control. Here $\tau_{pc}\times|d\beta_p/dt|$ should remain below a maximum, where τ_{pc} is the characteristic response time of the radial position control, determined by the typical poloidal field coil response and the penetration of the field provided by these coils through the vessel. At ITER, τ_{pc} is of the order of several seconds, dominated by the response of the poloidal field coil system, whilst in most present

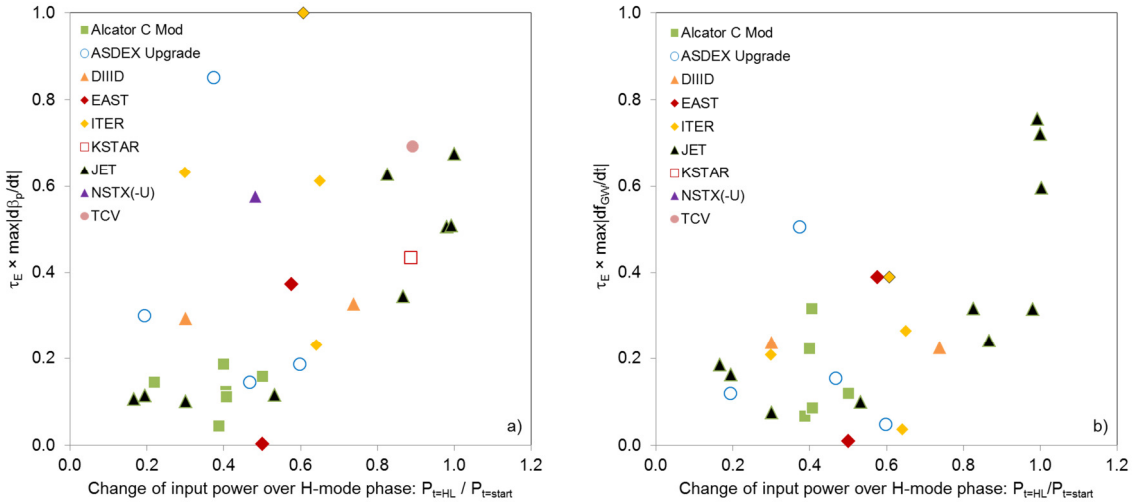

FIG. 8: *a) The peak change (i.e. decrease) in β_p, at the time of the H-L transition, normalized to $<\tau_E>$ (averaged over the duration of the H-L transition). b) The peak change in f_{GW}, at the time of the H-L transition, again normalized to the same $<\tau_E>$. Note that in both graphs the ITER points represent the assumed changes.*

day devices it may be determined by the vessel penetration time. Of course the maximum will depend on details, such as the plasma proximity to the inner wall, at the time of the H-L transition, and larger values are allowed for smaller plasmas.

The development of ℓ_i, relevant to VS, is related to both the current ramp-down rate and the $\tau_{L/R}$. Figure 3 has been shown that the latter can vary significantly over the duration of the termination. Therefore, $\tau_{L/R}$ averaged over the first half of the current ramp-down, when comparing this time-scale with current decay time in each device, as shown in figure 2b. It can be observed that for the case of a natural current decay in ITER, this ratio is, as expected, near unity.

Also a few of the Alcator C-Mod terminations have a current decay time of the same order as the L/R time. This means that for these cases, the current ramp-down is slower than the resistive time, τ_R, which is a fraction (~0.3-0.5) of $\tau_{L/R}$ [7,8]. Thus for these cases, the internal current density distribution is in equilibrium and follows the redistribution of the resistivity during the ramp-down (i.e. temperature profile changes). On the other hand, for other entries, the current ramp-down is faster than τ_R, and one expects a non-equilibrium situation. Changes in ℓ_i are driven by the current ramp-down itself. The faster, more typical, ITER terminations fall in the last category. Figure 9 shows the absolute change in ℓ_i, over the first half of the current ramp-down, as a function of the current ramp-down time normalized to $\tau_{L/R}$

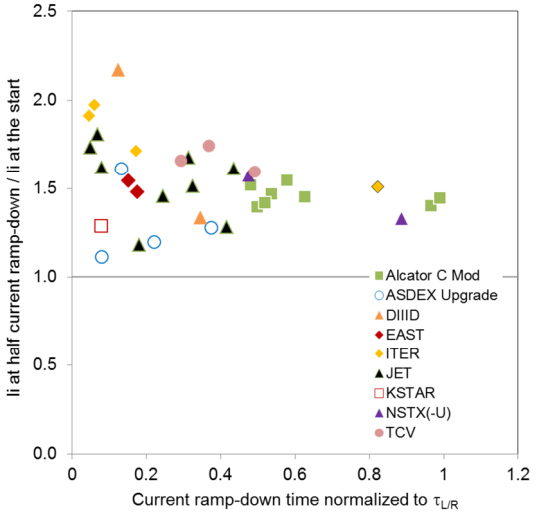

FIG. 9: Existence diagram of the relative change in ℓ_i over half the current ramp-down versus the ratio of the averaged current decay time and $\tau_{L/R}$

6. Recommendations

The database, built using a selected set of experimental termination cases, showed many similarities in the particle dynamics and current density behavior. Differences are found in relation to the specific control and heating capabilities of each device. Relevant for ITER is to maintain vertical, radial position, and shape control during the termination, especially at the time of the relatively fast H-L transition. The task is to show that the specific ITER design features allow a stable well-controlled termination. This is a joint effort in control, exception handling development and physics modelling

[10,11]. The results from this analysis can be used to better prescribe the inputs for the detailed modelling and preparation of ITER termination scenarios.

Present day devices can provide significant input power during a large fraction of the current ramp-down, keeping the plasma in H-mode and slowing down the increase in ℓ_i. The auxiliary power available at ITER limits this capability. Especially for a termination with a significant fraction of α-power, the ramp-down of the input power compared to the current is relatively fast, hence it is difficult to maintain H-mode and control the H-L transition. To maintain VS, a strong reduction in elongation during the ITER current ramp-down is essential. As a consequence, ITER terminations remain longer than present day devices at lower q_{95} and trace the upper boundary of the ℓ_i-q stability diagram. The impact on the MHD stability for such terminations needs to be assessed. This situation may be different when terminating an ITER H-mode without a larger fraction of α-power, for example at I_p=7.5MA.

The decay of the density and exhaust of the particle inventory, for such large size plasmas as in ITER, is sometimes perceived as problematic. However, the average required exhaust (in particles per second) decreases towards larger devices because the termination duration ($\sim\tau_{L/R}$) increases more than particle inventory ($\sim n_{GW}\times$Volume). The database entries showed that the density decay in H-mode is slower than that of the plasma current. The decay of the H-mode density can be seen as a change in the overall particle confinement or one could view it as a decay of specifically the pedestal density, when the current is ramped down. From the H_{98y2} confinement scaling one would expect the confinement to decay proportional to I_p [13]. Similarly the pedestal pressure is expected to decay by $\sim I_p^2$, hence the density and temperature can be assumed to scale approximately linear with I_p [14]. However, both the scalings are valid for steady-state situations and may not apply during the current ramp-down. The consequential rise in f_{GW} will limit the duration of the H-mode phase during the current ramp-down, hence putting a strong emphasis on the reduction in elongation to provide VS.

ITER terminations will benefit from controlled H-L transitions and this phase should be studied experimentally in more detail and properly modelled. The database cases all showed an H-L transition duration of the order of a several times τ_E. The timing H-L transition depends both on the radiation and value of dW/dt, the latter being able to substantially increase the total power flowing through the separatrix during a termination. The radiation levels relate to the methods of density and impurity control, which deserve further attention in the context of this joint analysis task.

Acknowledgements

ITER is a Nuclear Facility INB-174. This material is based in work using; the National Magnetic Confinement Fusion Program of China (No.2015GB102000), DoE Office of Science user Facilities Alcator C-Mod, NSTX, and DIII-D, supported by DoE Awards DE-FC02-99ER54512, DE-AC02-76CH03073, DE-FC02-04ER54698, respectively, the MSIP Fusion Program KSTAR and the framework of the EUROfusion Consortium and received funding from the Euratom research and training program 2014-2018 under grant agreement No 633053. The views and opinions expressed herein do not necessarily reflect those of the ITER Organization or the European Commission.

References

[1] SIPS, A.C.C., et al., Nucl. Fusion **49** (2009) 085015.
[2] POLITZER, P.A., et al., Nucl. Fusion **50** (2010) 135011
[3] KESSEL, C.E., et. al., Nucl. Fusion **53** (2013) 093021.
[4] LEHNEN, M, et al., Journ. Nucl. Mat. **463** (2015) 748.
[5] GRIBOV, Y, et al, Proc. of the EPS conf. on Plasma Physics 2016 (Leuven, Belgium)
[6] LOARTE, A., et al., Nucl. Fusion **54** (2014) 123014.
[7] MIKKELSEN, D.R., Phys. Fluids B **1** (1989) 333.
[8] LUCE, T.C., et al., Nucl. Fusion **45** (2005) S86.
[9] HUMPHREYS, D, et al., Nucl. Fusion (2009) 115003.
[10] HUMPHREYS, D, et al., Proc. of this IAEA FEC (EX/P6-37)
[11] GREENWALD, M, Plasma Phys. Control. Fusion **44** (2002) R27.
[12] SNIPES, J.A., et al., Proc. of this IAEA FEC (EX/P6-36)
[13] MCDONALD, D.C., et al., Nucl. Fusion **47** (2007) 147.
[14] SNYDER, P.B., et al., Phys. Plasmas **16** (2009) 056118.